MAGNETIC RESONANCE IMAGING OF THE CANINE BRAIN AT 3 AND 7 T

Paula Martín-Vaquero, Ronaldo C. da Costa, Rita L. Echandi, Christina L. Tosti, Michael V. Knopp, Steffen Sammet

Magnetic resonance (MR) imaging of the canine brain is commonly acquired at field strengths ranging from 0.2 to 1.5 T. Our purpose was to compare the MR image quality of the canine brain acquired at 3 vs. 7 T in dogs. Low-resolution turbo spin echo (TSE) T2-weighted images (T2W) were obtained in transverse, dorsal, and sagittal planes, and high-resolution TSE T2W and turbo spin echo proton density-weighted images were obtained in the transverse and dorsal planes, at both 3 and 7 T. Three experienced reviewers evaluated 32 predetermined brain structures independently and without knowledge of field strength for spatial resolution and contrast. Overall image quality and evidence of artifacts were also evaluated. Contrast of gray and white matter was assessed quantitatively by measuring signal intensity in regions of interest for transverse plane images for the three pulse sequences obtained. Overall, 19 of the 32 neuroanatomic structures had comparable spatial resolution and contrast at both field strengths. The overall image quality for low-resolution T2W images was comparable at 3 and 7 T. High-resolution T2W was characterized by superior image quality at 3 vs. 7 T. Magnetic susceptibility and chemical shift artifacts were slightly more noticeable at 7 T. MR imaging at 3 and at 7 T provides high spatial resolution and contrast images of the canine brain. The use of 3 and 7 T MR imaging may assist in the elucidation of the pathogenesis of brain disorders, such as epilepsy. © 2010 *Veterinary Radiology & Ultrasound, Vol. 52, No. 1, 2011, pp 25–32.*

Key words: 7.0 T, brain, dog, MR, MRI.

Introduction

Magnetic resonance (MR) imaging is the modality of choice for evaluating the brain parenchyma due to its superior soft-tissue contrast. It is the gold-standard for imaging the central nervous system in human patients and animals.[1–4] The routine clinical availability of MR imaging for human patients began in the mid-1980s.[5] Since then, optimization and improvement of MR units has been a continuous effort and scanners for human imaging up to 9.4 T can be found today.[6]

At present, only a limited number of institutions have commercial 7 T MR scanners.[7] The use of higher field strengths has allowed the visualization of brain lesions that were not evident at lower field strength, and has helped achieve a better understanding of some of the most common neurologic disorders in people, such as multiple sclerosis, cerebrovascular accidents, or epileptic syndromes.[5,7–12]

Most MR systems used for veterinary patients range from 0.2 to 1.5 T.[13–16] Higher field strength MR imaging is a fairly new and unexplored area in veterinary medicine, although some information from imaging at 3 T is available.[17] There is a paucity of information documenting the use of field strengths >3 T for imaging of the canine brain.[18,19]

The purpose of this study was to qualitatively and quantitatively compare MR images of the brain of clinically normal dogs using a 3 and 7 T units. We hypothesized that MR imaging of the normal canine brain at 7 T would yield superior spatial resolution and contrast compared with the images acquired at 3 T.

Materials and Methods

Four healthy intact male purpose bred Beagle dogs were imaged. Body weight and age ranged from 10.5 to 12 kg (mean 11.2 kg) and from 1.3 to 3 years (mean 2.1 years). All dogs were normal with no evidence of neurologic disease. Results of complete blood counts and serum chemistry profiles were normal for all dogs.

Dogs were premedicated with intramuscular acepromazine and hydromorphone. General anesthesia was induced with intravenous propofol and maintained with isoflurane using assisted mechanical ventilation.

Each dog underwent MR imaging at 3 T* and 7 T† in random order on the same day and under one anesthetic procedure. The dogs were in sternal recumbency with the head centered in the coil. Three fiducial

From the Department of Veterinary Clinical Sciences, College of Veterinary Medicine, The Ohio State University, Columbus, OH (Martín-Vaquero, da Costa, Echandi); the Department of Radiology, The Ohio State University Medical Center, Columbus, OH (Tosti, Knopp and Sammet).

Dr. Martín-Vaquero was sponsored by Obra Social "la Caixa" Fellowship Program of Spain. An abstract of the study was presented in the Annual Forum of the American College of Veterinary Internal Medicine (ACVIM Forum) in Anaheim, California in June 2010.

Address correspondence and reprint requests to Ronaldo C. da Costa, at the above address. E-mail: dacosta.6@osu.edu

Received February 28, 2010; accepted for publication July 25, 2010.
doi: 10.1111/j.1740-8261.2010.01747.x

*Achieva 3.0 Tesla, Philips Healthcare, Best, the Netherlands.
†Achieva 7.0 Tesla, Philips Healthcare.

TABLE 1. Summary of 3 and 7 T MR Imaging Parameters

Pulse Sequence	Low-Resolution T2W		High-Resolution T2W		PDW	
Magnetic field strength (Tesla)	3	7	3	7	3	7
Echo time (TE, ms)	80	80	80	80	15	15
Repetition time (TR, ms)	3000	5500	3000	5500	2000	3000
NEX	1	1	1	1	2	2
Slice thickness (mm)	3	3	2	2	2	2
Interslice gap (mm)	0	0	0	0	0	0
FOV (mm)						
Transverse plane	120 × 120*	120 × 120*	80 × 120	80 × 120	120 × 100	120 × 100
Dorsal plane	120 × 100.7	120 × 100.7	80 × 100	80 × 100	120 × 142	120 × 142
Acquisition matrix						
Transverse plane	224 × 210*	224 × 224*	268 × 396	268 × 400	240 × 198	240 × 198
Dorsal plane	224 × 180	224 × 176	268 × 324	268 × 320	240 × 282	240 × 282
Acquisition time (min:s)						
Transverse plane	01:30†	04:07†	05:06	11:55	08:52	13:18
Dorsal plane	01:28	03:18	02:48	07:42	12:36	09:27

*Same FOV and matrix also used for low-resolution T2W in the sagittal plane. †Same acquisition time for low-resolution T2W in the sagittal plane. T2W, T2-weighted images; PDW, proton density-weighted images; MR, magnetic resonance.

markers‡ were used. One was on the skin immediately dorsal to the most caudal end of the occipital crest and two others were on the skin over the end of the left and right zygomatic arches, respectively. The fiducial markers were used to guide slice positioning during the acquisition of scout images.

Low-resolution turbo spin echo T2-weighted images (TSE T2W) of the brain were obtained in transverse, sagittal, and dorsal planes. High-resolution TSE T2W and turbo spin echo proton density-weighted (TSE PDW) images were acquired in transverse and dorsal planes. All sequences were obtained for all dogs at both 3 and 7 T. Transverse images were oriented perpendicular to the hard palate. Dorsal and sagittal images were obtained perpendicular to the transverse plane. Images at 3 T were acquired using an eight-channel receive-only phased array extremity coil designed for the human knee. Images at 7 T were acquired with a transmit-receive quadrature human extremity coil.

MR imaging protocols had been optimized for both field strengths before the investigation was started to define the best imaging parameters for the sequences of interest. Two Beagle dogs of similar age and size to the dogs imaged in this study were used for the optimization. A total of 12 h of scanning time was used to define the protocol. To achieve a fair comparison between field strengths, the imaging protocols were kept as similar as possible (Table 1).

Qualitative and quantitative image assessment was performed. Images were reviewed using dedicated software.§ Qualitative evaluation of the images was performed by a board-certified veterinary neurologist (R.C.dC.), a board-certified veterinary radiologist (R.E.). and a physician (S.S.) experienced in neuroimaging. Images were evaluated independently and without knowledge of field strength. Before review, the images had been organized by a fourth investigator (P.M.V.), who was aware of the information regarding the dog, field strength, pulse sequence, image plane, and slice. Using dedicated imaging

TABLE 2. Anatomical Structures Qualitatively Assessed at 3 and 7 T (per Pulse Sequence and Image Plane)

- Transverse plane
  - T2-weighted images (T2W, low and high resolution)
    - Level of rostral medulla/cochlea
      - Cerebellar vermis
      - Middle cerebellar peduncle
    - Level of thalamus/temporomandibular junction
      - Hippocampus
      - Piriform lobe
      - Cortical gray matter (GM) and white matter (WM) contrast
    - Level of optic chiasm/caudate nuclei
      - Caudate nuclei
      - Corpus callosum
      - Cyngulate gyrus
      - Cortical GM and WM contrast (centrum semiovale)
    - Level of frontal lobe
      - GM and WM contrast on cortical area
  - Proton density-weighted images (PDW)
    - Level of thalamus/temporomandibular junction
      - Costical GM and WM contrast
    - Level of optic chiasm/caudate nuclei
      - Caudate nuclei
      - Corpus callosum
      - Cyngulate gyrus
      - Cortical GM and WM contrast (centrum semiovale)
- Dorsal plane
- T2W (low and high resolution) and PDW
  - Precruciate and postcruciate gyri
  - Cortical GM and WM contrast in the region of temporal/occipital lobe area
- Sagittal plane
  - T2W (low resolution)
    - Cerebellar GM and WM contrast

‡Vitamin E 400 capsules. Schiff, Schiff Nutrition International, Salt Lake City, UT.

§E-film Merge Healthcare, Milwaukee, WI.

software, the image pair (3 vs. 7 T) of each dog and each combination of pulse sequence, image plane, and anatomic location was displayed side-by-side using 21.3 in. monitors approved for diagnostic quality.¶

Qualitative evaluation of the images consisted of (1) subjective assessment of spatial resolution (ability to distinguish two objects as separate entities as they become closer together) and contrast (ability to distinguish separate objects based on differences in magnitude of signal or intensity relative to the different shades of gray) of a given list of 32 neuroanatomic structures (Table 2), (2) subjective assessment of overall image quality, and (3) evaluation of the presence or absence of artifacts. Images were evaluated in a caudal to rostral fashion. All neuroanatomical structures were identified by referring to anatomic texts and published atlases.[3,13,20–22] Spatial resolution and contrast of the structures were evaluated subjectively using a three-point grading system: left image with superior spatial resolution and contrast = 1, left and right images with equal spatial resolution and contrast = 2, right image with superior spatial resolution and contrast = 3. As there were four dogs studied and three investigators reviewing the images, each anatomic structure was evaluated a total of 12 times. To decide if a structure had superior spatial resolution and contrast at a specific magnetic field strength, a cut-off value of more than 50% of the evaluations (i.e., more than six times) was established. All anatomic structures were assigned to one of the following groups, provided they were considered to have superior spatial resolution and contrast using the same magnet in more than six occasions: (1) anatomic structures with superior spatial resolution and contrast at 3 T, (2) structures with superior spatial resolution and contrast at 7 T, or (3) structures which did not reach the cut-off value at either magnetic field strength or had been considered to have comparable image spatial resolution and contrast at both 3 and 7 T in more than six occasions.

The overall image quality was evaluated subjectively for low- and high-resolution T2W transverse images. In this instance, the paired low- or high-resolution T2W pulse sequences (3 vs. 7 T) were displayed side-by-side. The reviewers were able to scroll through the complete series of slices for the given pulse sequence to evaluate subjectively which specific magnetic strength had superior overall image quality. The same three-point scale described previously was used in this evaluation.

The presence of artifacts was recorded and scored subjectively for low- and high-resolution T2W transverse images. The reviewers were instructed to look for magnetic susceptibility artifacts, which cause areas of signal void at air-tissue interfaces; and chemical shift artifacts, which

¶Eklin-branded/WIDE USA Corporation 3-MegaPixel diagnostic flat panel monitor, model PGL21, Carlsbad, CA.

TABLE 3. Anatomical Structures Visualized with Superior Spatial Resolution and Contrast at 3 T, at 7 T or Comparable at 3 and 7 T, respectively

- Superior image resolution and contrast at 3 T
  - T2-weighted images (T2W) low resolution
    - Transverse plane
      - Cortical gray matter (GM) and white matter (WM) contrast (level of thalamus/temporomandibular junction)
  - T2W high resolution
    - Transverse plane
      - Cortical GM and WM contrast (level of the thalamus/temporomandibular junction)
      - Cyngulate gyrus
      - Cortical GM and WM contrast at the level of the optic chiasm/caudate nuclei (centrum semiovale)
  - Proton density-weighted images (PDW)
    - Transverse plane
      - Cortical GM and WM contrast (level of the thalamus/temporomandibular junction)
- Superior image resolution and contrast at 7 T
  - T2W low resolution
    - Transverse plane
      - Cerebellar vermis
    - Dorsal plane
      - Precruciate and postcruciate gyri
      - Cortical GM and WM contrast (level of temporal/occipital area)
  - T2W high resolution
    - Dorsal plane
      - Cortical GM and WM contrast (region of temporal/occipital area)
  - PDW
    - Transverse plane
      - Caudate nuclei
      - Corpus callosum
      - Cortical GM and WM contrast (level of the optic chiasm/caudate nuclei—centrum semiovale)
    - Dorsal plane
      - Cortical GM and WM contrast (region of temporal/occipital area)
- Comparable image resolution at 3 and 7 T
  - T2W low resolution
    - Transverse plane
      - Middle cerebellar peduncle
      - Hippocampus
      - Piriform lobe
      - Caudate nuclei
      - Corpus callosum
      - Cyngulate gyrus
      - Cortical GM and WM contrast at the level of the optic chiasm/caudate nuclei (centrum semiovale)
      - Cortical GM and WM contrast at the level of the frontal lobe
    - Sagittal plane
      - Cerebellar GM and WM contrast
  - T2W high resolution
    - Transverse plane
      - Cerebellar vermis
      - Middle cerebellar peduncle
      - Hippocampus
      - Piriform lobe
      - Caudate nuclei
      - Corpus callosum
      - Cortical GM and WM contrast at the level of the frontal lobe
    - Dorsal plane
      - Precruciate and postcruciate gyri
  - PDW
    - Transverse plane
      - Cyngulate gyrus
    - Dorsal plane
      - Precruciate and postcruciate gyri

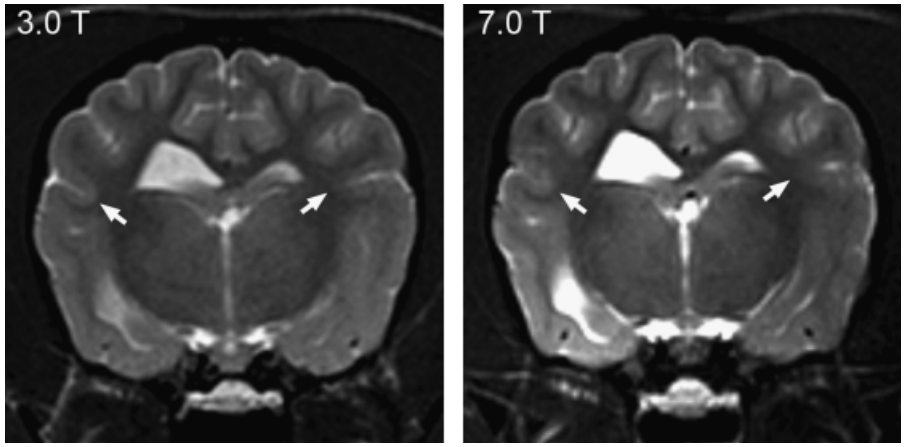

FIG. 1. Transverse low-resolution T2-weighted images at the level of the thalamus/temporomandibular junction. Note the superior cortical gray and white matter spatial resolution and contrast (white arrows) at 3 T.

occur and fat-tissue interfaces and can give rise to artificial lines superimposed over the tissues. Scores for the presence of artifacts were the following: 0 = absent, 1 = mild, 2 = moderate, 3 = severe.

The quantitative assessment of the images was based on signal intensity measurements in regions of interest (ROIs) to measure the contrast of gray matter and white matter. ROIs of gray matter and white matter were obtained for the three pulse sequences for transverse images at the level of the optic chiasm/caudate nuclei. One ROI each of gray matter and white matter were obtained per pulse sequence and magnetic field strength for all dogs. The ROIs covered 4 pixels and were manually placed by the same author (P.M.V.) for all images analyzed to minimize interpersonal influence on ROI placement. For every dog, the ROI over the white matter was lateral to the most dorsal aspect of the caudate nuclei. The ROI over the gray matter was located laterally at the same level of the white matter ROI, in between the gyri and sulci at that level in the cerebral cortical gray matter. The following normalized gray–white matter contrast ratio was calculated: $100 \times \{(\text{gray matter} - \text{white matter})/\text{gray matter}\}$. Mean values and standard deviation on the mean values were calculated for both magnetic field strengths. Statistical analyses of the ROIs mean values were obtained using a paired two-sample Student's *t*-test. Analyses were performed using dedicated computer software.‖ Significance was set at $P < 0.05$.

Results

All dogs were successfully imaged at 3 and 7 T.

Results of qualitative evaluation of the neuroanatomic structures are summarized in Table 3. There were five neuroanatomic structures that were characterized by superior spatial resolution and contrast at 3 T, whereas eight structures had superior spatial resolution and contrast at 7 T. Nineteen out of the 32 structures were characterized by comparable spatial resolution and contrast on 3 and 7 T images. Images at 3 T had superior spatial resolution and contrast of the cortical gray matter and white matter at the level of the thalamus/temporomandibular junction on transverse images for all three sequences (Fig. 1). Gray matter and white matter spatial resolution and contrast in the temporal/occipital cortical area were consistently better at 7 T on dorsal plane images for the three pulse sequences (Fig. 2). Seventeen out of 25 anatomic structures evaluated on T2W images, such as the hippocampus, piriform lobe, caudate nuclei, or corpus callosum, had comparable spatial resolution and contrast at 3 and 7 T. Some structures, such as the cerebellar gray matter and white matter evaluated on sagittal images, had comparable or superior spatial resolution and contrast at 7 T than at 3 T (Fig. 3), although in this instance the minimum cut-off value was not reached. Four out of seven anatomic structures evaluated on PDW images had superior image spatial resolution and contrast at 7 T than at 3 T (Fig. 4).

Overall image quality for low-resolution T2W was comparable at 3 and 7 T. With the high-resolution T2W images, there was superior overall image quality at 3 T (Fig. 5).

There were mild magnetic susceptibility and chemical shift artifacts at 3 T. These artifacts were moderate on images acquired at 7 T. Magnetic susceptibility artifacts, identified as a signal void or signal drop, were noted at both field strengths when evaluating the dorsal aspect of the frontal lobe area in the transverse plane images (Fig. 6). These artifacts partially obscured visualization of the most dorsal aspect of the frontal lobe parenchyma. Chemical shift artifacts, which could be identified as an artificial

‖GraphPad Software, GraphPad Software Inc., La Jolla, CA.

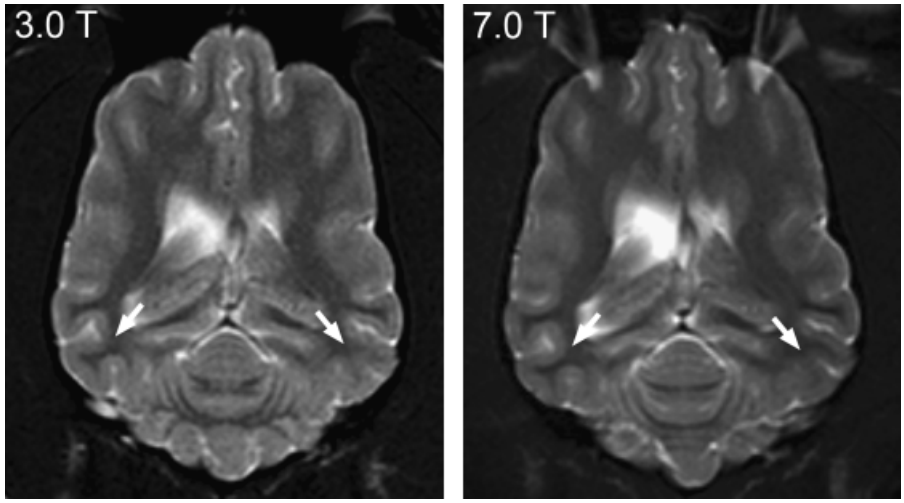

FIG. 2. Dorsal low-resolution T2-weighted images at the level of the occipital/temporal area. Note the superior cortical gray and white matter contrast (white arrows) at 7 T.

hyperintense line superimposed over the most dorsal aspect of the brain parenchyma, were also seen at both magnetic field strengths, slightly more noticeable at 7 T than at 3 T (Fig. 7).

Quantitatively, the mean gray and white matter contrast was higher at 7 T. However, the difference was not statistically significant (low-resolution T2W [$P = 0.329$], high-resolution T2W [$P = 0.351$], and PDW [$P = 0.179$]) for any pulse sequence obtained (Table 4).

Discussion

We evaluated, both qualitatively and quantitatively, MR images of the brain of clinically normal dogs acquired at 3 and 7 T. The goal was to assess the cerebellum and different regions of the cerebrum. Of 32 anatomic structures evaluated, 19 had comparable spatial resolution and contrast at 3 and 7 T. The structures were chosen based on their functional importance, use as anatomic landmarks or because of a relation to common neural disease. Special importance was given to anatomic structures that conform the thalamocortex, which are known to be the areas of the brain where seizure activity originates and spreads, both in humans and dogs.[5,20,21,23] Idiopathic epilepsy is the most common cause of recurrent seizures in dogs.[20,23] To date, canine idiopathic epilepsy is not associated with any MR imaging abnormalities.[23] In human epileptic syndromes, the rapid advances made in MR imaging enable more subtle lesions to be detected.[5,8,10,24–26]

Our hypothesis of 7 T images having superior spatial resolution and contrast was not confirmed for the majority of the structures assessed. This may be due to limitations regarding equipment and imaging protocols at 7 T.[7,8,18,27] With increasing magnetic field strength, several physical features change, including signal-to-noise ratio (SNR), T1 and T2 relaxation time, chemical shift, and radiofrequency deposition.[8] The SNR increases almost linearly with field strength,[7,8] providing better image quality.[2,7,8] Other field strength-dependent changes can be disadvantageous, such as increased chemical shift artifact, and these need to be compensated by modification of the imaging technique.[8] Chemical shift increases in proportion to the magnetic field

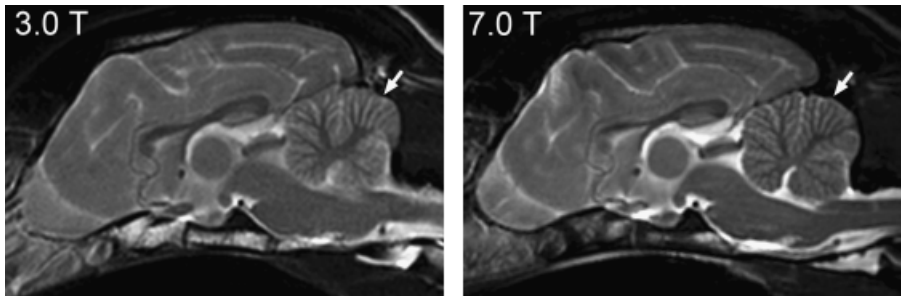

FIG. 3. Sagittal low-resolution T2-weighted images at the level of the interthalamic adhesion. Note the cerebellar gray and white matter contrast (white arrow), which was considered to have comparable or superior spatial resolution and contrast at 7 T than at 3 T.

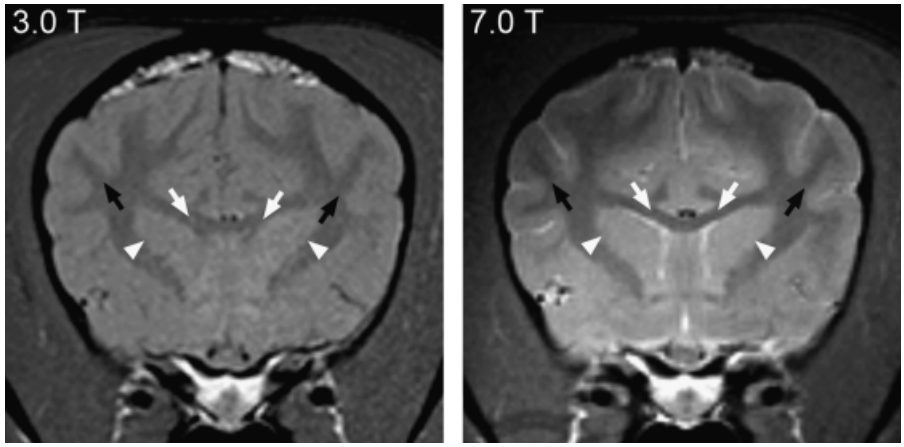

FIG. 4. Transverse proton density-weighted images at the level of the optic chiasm/caudate nuclei. The caudate nuclei (white arrowheads), corpus callosum (white arrows), and cortical gray and white matter (black arrows) are characterized by superior spatial resolution and contrast at 7 T.

and it can cause pronounced artifacts at fat-tissue interfaces. However, the use of a higher receiver bandwidth can help minimize this artifact.[8]

For human clinical MR imaging, the consensus is that 3 T scanners have a two-fold SNR advantage over 1.5 T systems.[7] Similarly, scanning at 7 T compared with 3 T could more than double the SNR even further.[7] SNRs were not calculated in this study because the 3 T coil was a phased array coil with a nonuniform noise distribution, making the computation of SNR based on ROIs invalid. SNR could be calculated for these imaging sequences only with the addition of a noise map, but this sequence was not available on our scanner at the time.

The use of 3 and 7 T MR imaging in human neurology has been proven to be advantageous over conventional 1.5 T scanners for allowing visualization of a higher number of lesions in people with multiple sclerosis[7,9,11] or improving the identification of cortical brain abnormalities in epileptic patients.[7,8,10] Scanners such as the 7 T unit in this study are still used primarily for research.[7,11,12]

The difference in coil design between 3 and 7 T was a limitation, because even phased array coils for these two systems cannot be designed in exactly the same way. Moreover, in canine MR imaging at 7 T there is little information available regarding imaging protocols[18,19] and information needs to be extrapolated from what is currently used at 1.5 or 3 T. We kept the imaging protocols as similar as possible. This might have limited the performance of an individual scanner, but every attempt was made to make the comparison as reasonable as possible given the knowledge and equipment available.

Although there was higher mean gray and white matter contrast for the 7 T images, the lack of statistical significance was likely due to the small sample size.

The high-resolution T2W images were considered to have superior overall image quality at 3 T than at 7 T,

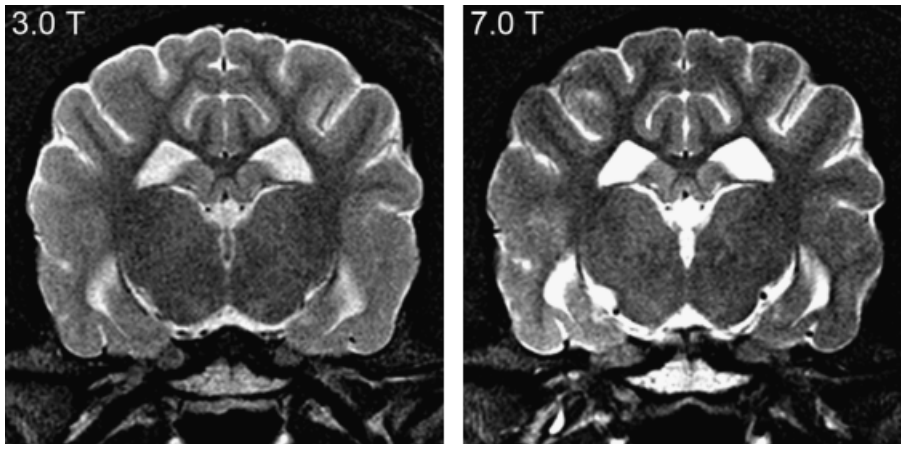

FIG. 5. Transverse high-resolution T2-weighted images at the level of the thalamus/temporomandibular junction. Note the superior overall image quality at 3 T vs. the noisier appearance of the 7 T image.

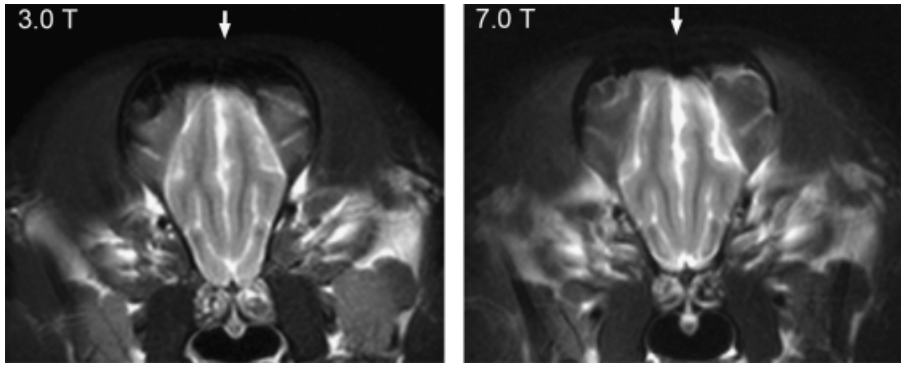

FIG. 6. Transverse low-resolution T2-weighted images at the level of the frontal lobe. Note the susceptibility artifacts on the dorsal aspect of the frontal lobe (white arrows), which appear as a signal void within the magnetic resonance image. These were slightly more pronounced at 7 T than at 3 T.

due to an overall noisier appearance at 7 T. This was considered to decrease overall image quality, even if there was good spatial resolution and contrast. Because imaging parameters directly relate to signal and spatial resolution, they were kept identical to obtain high-resolution T2W images both at 3 and 7 T. The noisier appearance at 7 T was likely related to the difference in coil design between the coils used for this study.

Subjectively, there was more evidence of magnetic susceptibility and chemical shift artifacts at 7 T compared with 3 T. Higher field MR units, such as 7 T, have an intrinsic propensity for certain imaging artifacts, such as magnetic susceptibility artifacts.[7,8,18] These artifacts occur at interfaces between substances with different susceptibility values, such as air-tissue.[28] In our study, susceptibility artifacts were noted at both field strengths when evaluating the frontal lobe area in transverse images, but were more noticeable at 7 T. This is likely related to the nearly linear increase in susceptibility effects with field strength.[8] The air-filled frontal sinuses cause distortion of the magnetic field, producing an area of signal void in the frontal lobe parenchyma. This artifact is noted commonly in people at 7 T MR. New equipment is being developed to attempt to improve the performance of 7 T head coils over this region.[27]

Chemical shift artifacts were noted at both field strengths but were slightly more conspicuous at 7 T. Protons residing in different molecular environments have a slightly different resonant frequency. This is referred to as

TABLE 4. ROIs Comparing White Matter (WM) and Gray Matter (GM) Image Contrast for Each Pulse Sequence at 3 and 7 T (Ratio = 100 × (GM−WM)/GM)

	Low-Resolution T2W (Tesla)		High-Resolution T2W (Tesla)		PDW (Tesla)	
	3 (%)	7 (%)	3 (%)	7 (%)	3 (%)	7 (%)
Dog 1	32.0	26.7	26.0	30.3	20.5	19.0
Dog 2	26.6	32.5	29.3	34.6	18.6	21.0
Dog 3	33.3	43.1	43.3	42.0	22.0	30.4
Dog 4	30.5	35.0	32.4	31.6	20.3	25.8
Mean	30.6	34.3	32.7	34.6	20.3	24.0
SD on mean	2.90	6.80	7.50	5.23	1.39	5.10
P-value*	0.329		0.351		0.179	

*Paired two-sample *t*-test for a difference in mean.T2W, T2-weighted images; PDW, proton density-weighted images; ROI, region of interest.

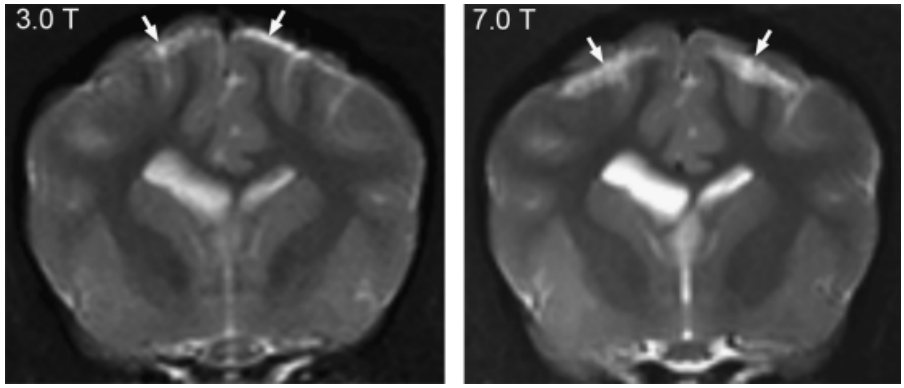

FIG. 7. Transverse low-resolution T2-weighted images at the level of the caudate nuclei. Note the chemical shift artifacts (i.e., fat-water shift artifacts) on the dorsal aspect of the brain (white arrows), which appear as an artificial hyperintense line superimposed over the most dorsal aspect of the brain parenchyma. Chemical shift artifacts were slightly more pronounced at 7 T than at 3 T.

chemical shift and it can cause pronounced artifact at fat-tissue interfaces.[8,28] In our study, chemical shift artifacts were noted on the most dorsal aspect of the head on transverse images. Chemical shift increases in proportion to the magnetic field strength.[8]

Based on our results, imaging of the canine brain at 3 and 7 T provides images with comparable spatial resolution and contrast for most anatomic structures. At this time, with the current imaging protocols and equipment available, brain imaging at 7 T does not seem to provide a substantial improvement vs. imaging at 3 T. However, the promising results obtained in people at 7 T suggest that once 7 T imaging becomes more readily available and the technical difficulties are overcome, it may also provide superior image quality in veterinary patients and help to further characterize canine brain disorders.

REFERENCES

1. Farrow CS, Tryon K. Fathoming the mysteries of magnetic resonance imaging. J Am Anim Hosp Assoc 2000;36:192–198.
2. Sage JE, Samii VF, Abramson CJ, et al. Comparison of conventional spin-echo and fast spin-echo magnetic resonance imaging in the canine brain. Vet Radiol Ultrasound 2006;47:249–253.
3. Leigh EJ, Mackillop E, Robertson ID, et al. Clinical anatomy of the canine brain using magnetic resonance imaging. Vet Radiol Ultrasound 2008;49:113–121.
4. Gavin PR, Bagley RS. Practical small animal MRI, 1st ed. Ames, IA: Wiley-Blackwell, 2009.
5. Kuzniecky RI, Jackson GD. Magnetic resonance in epilepsy: neuroimaging techniques, 2nd ed. San Diego, CA: Elsevier Academic Press, 2005.
6. Vaughan T, DelaBarre L, Snyder C, et al. 9.4T human MRI: preliminary results. Magn Reson Med 2006;56:1274–1282.
7. Kangarlu A. High-field magnetic resonance imaging. Neuroimag Clin N Am 2009;19:113–128.
8. Kuhl CK, Träber F, Schild HH. Whole-body high-field strength (3.0-T) MR imaging in clinical practice. Part I. Technical considerations and applications. Radiology 2008;246:675–696.
9. Sicotte NL, Voskuhl RR, Bouvier S, et al. Comparison of multiple sclerosis lesions at 1.5 and 3.0 Tesla. Invest Radiol 2003;38:423–427.
10. Phal PM, Usmanov A, Nesbit GM, et al. Qualitative comparison at 3-T and 1.5-T MRI in the evaluation of epilepsy. Am J Roentgenol 2008;191:890–895.
11. Tallantyre E, Morgan PS, Dixon JE, et al. A comparison of 3T and 7T in the detection of small parenchymal veins within MS lesions. Invest Radiol 2009;44:491–494.
12. Conijn MM, Hendrikse J, Zwanenburg JJ, et al. Perforating arteries originating from the posterior communicating artery: a 7.0 Tesla MRI study. Eur Radiol 2009;19:2986–2992. Available at http://www.springerlink.com/content/m1n877787k174067/ (accessed September 1, 2009).
13. Kraft SL, Gavin PR, Wendling LR, et al. Canine brain anatomy on magnetic resonance images. Vet Radiol Ultrasound 1989;30:147–158.
14. Viitmaa R, Cizinauskas S, Bergamasco LA, et al. Magnetic resonance imaging findings in Finnish Spitz dogs with focal epilepsy. J Vet Int Med 2006;20:305–310.
15. Smith PM, Talbot CE, Jeffery ND. Findings on low-field cranial MR images in epileptic dogs that lack interictal neurological deficits. Vet J 2008;176:320–325.
16. McConnell JF, Garosi L, Platt SR. Magnetic resonance imaging findings of presumed cerebellar cerebrovascular accident in twelve dogs. Vet Radiol Ultrasound 2005;46:1–10.
17. Rodriguez D, Rylander H, Vigen KK, et al. Influence of field strength on intracranial vessel conspicuity in canine magnetic resonance angiography. Vet Radiol Ultrasound 2009;50:477–482.
18. Kang BT, Ko KJ, Jang DP, et al. Magnetic resonance imaging of the canine brain at 7 T. Vet Radiol Ultrasound 2009;50:615–621.
19. Kang MH, Lim CY, Park C, et al. 7.0-Tesla Tesla magnetic resonance imaging of granulomatous meningoencephalitis in a Maltese dog: a comparison with 0.2 and 1.5-Tesla. J Vet Med Sci 2009;71:1545–1548.
20. de Lahunta A, Glass E. Veterinary neuroanatomy and clinical neurology, 3rd ed. St. Louis, MO: Saunders Elsevier, 2009;6–22.
21. Jenkins TW. Functional mammalian neuroanatomy, 2nd ed. Philadelphia: Lea & Febiger, 1978;387–445.
22. Evans HE. Miller's anatomy of the dog, 3rd ed. Philadelphia: Saunders, 1993.
23. Chandler K. Canine epilepsy: what can we learn from human seizure disorders? Vet J 2006;172:207–217.
24. Bronen RA, Fulbright RK, Kim JH, et al. A systematic approach for interpreting MR images of the seizure patient. Am J Roentgenol 1997;169:241–247.
25. Berendt M, Gram L. Epilepsy and seizure classification in 63 dogs: a reappraisal of veterinary epilepsy terminology. J Vet Intern Med 1999;13:14–20.
26. Duncan JS. Imaging and epilepsy. Brain 1997;120:339–377.
27. Avdievich NI, Hetherington HP, Kuznetsov AM, et al. 7T head volume coils: improvements for rostral brain imaging. J Magn Reson Imaging 2009;29:461–465.
28. Arena L, Morehouse HT, Safir J. MR imaging artifacts that simulate disease: how to recognize and eliminate them. Radiographics 1995;15:1373–1394.